Non-shock Ignition Simulation for PBXs based on Combined Microcrack and Microvoid Hotspot Mechanisms

Kun Yang, Yanqing Wu*, Fenglei Huang
State Key Laboratory Explosion Science and Technology, Beijing Institute of Technology, Beijing 100081, China

1 Abstracts

A multiscale damage-ignition model incorporating two micro-defects related hotspot mechanisms, namely, shear-crack friction and void collapse, has been developed to evaluate non-shock ignition of polymer-bonded explosives (PBXs). For an uncovered PBX9501 charge punched by a flat-front rod, the simulated results show that shear-crack friction heating plays a critical role on ignition under low-velocity impact (<400m/s). Under high-velocity impact (>400m/s), the heating due to void collapse becomes to dominate ignition because time-to-ignition of void hotspots (~1μs) is shorter than the time of crack hotspots (~10μs). At the beneath of rod, the cracks are stable governed by friction-locked stress state and void collapse becomes a dominant hotspot mechanism. At the periphery of rod, both the shear-crack and void collapse hotspots have strong influences on ignition.

2 Introduction

Microstructural defects of polymer bonded explosives (PBXs), i.e., microcracks and microvoids, play a crucial role on the formation of hotspots of material, thereby significantly affecting the safety of PBXs in their transportation, storage, and application [1].

In the past, several defects related hotspot mechanisms, i.e., void collapse, crack friction heating, and heating at crack tips, have been proposed [2]. Idar et al. [3] conducted the modified Steven test for PBX9501 and found that the impact threshold for damaged sample shows a significant reduction compared to the pristine threshold. Borne et al. [4] suggested that intragranular voids between explosive crystal has a strong influence on the sensitivity of a kind of cast PBXs. Ravindran et al. [5] proposed that frictional heating of crystals and debonding of the binder are two possible hotspot mechanisms for a PBX simulant under dynamic loadings. However, the dominant mechanism is still indeterminate [6]. Thus, analysis of combined microcrack and microvoid related hotspot mechanisms is conducive to deeply understand the role of defects on ignition of PBXs.

Correspondence to: wuyqing@bit.edu.cn (Yanqing WU)

In the present work, a physical model which incorporates with combined microcrack and void hotspot mechanisms has been developed to describe the defects related ignition of PBXs. Damage and ignition responses of punched PBX samples were investigated based on combined micro-crack and void mechanisms.

3 Model Descriptions

A damage viscoelastic-plastic model which considers several possible evolution-modes of microcracks and microvoids (cracks: friction-locked, shear with friction, pure shear, mixed shear and open, and normal open; voids: collapse and distortion) has been developed in our previous works [7,8]. A brief summary of stress-strain relation of this model is presented. The literature should be referenced for full details of the model and its parameterization [7,8].

The deviatoric stress rate is described as,

$$\dot{\boldsymbol{s}} = 2GA\left(\dot{\boldsymbol{e}} - \dot{\boldsymbol{e}}^{p}\right) - B\boldsymbol{s} - \boldsymbol{C} \tag{1}$$

where $\boldsymbol{e}^{p}$ is the plastic deviatoric strain, A and B are function of mean crack radius; $\boldsymbol{C}$ is a function of the deviatoric stress component and relaxation time for the nth Maxwell element.

The pressure-volume relation in the solid is described by the Mie-Grüneisen EOS. The rate of pressure is obtained by,

$$\dot{P} = -K\dot{\varepsilon}_{v} + \Gamma_{s}\boldsymbol{s}\dot{\boldsymbol{e}} + \alpha\dot{\varepsilon}_{v}^{p} + \chi f k_{w}\omega\left(\sigma\right)\frac{\boldsymbol{s}\dot{\boldsymbol{e}}^{p}}{\sigma_{e}} \tag{2}$$

where K is the bulk modulus of the porous material, Γ_{s} is the Grüneisen coefficient, $\alpha = K - \left(1+\Gamma_{s}\right)P$, $\chi = K_{s} - \left(1+\Gamma_{s}\right)P_{s}$, $K_{s} \equiv \rho_{s}\left(\partial P_{s} / \partial \rho_{s}\right) + \Gamma_{s}P_{s}$.

The law of crack growth is expressed as,

$$\dot{\bar{c}} = \dot{c}_{\max}\left\langle 1 - \frac{2\bar{\gamma}}{g\left(\boldsymbol{\sigma}, \bar{c}\right)} \right\rangle \tag{3}$$

where $\dot{c}_{\max}$ is the maximum crack growth speed, $\bar{\gamma}$ is the effective surface energy, and $g\left(\boldsymbol{\sigma}, \bar{c}\right)$ is the energy-release rate.

The evolution of void fraction (f) is the additive of the void fraction change due to void collapse and void distortion,

$$\dot{f} = \left(1 - f\right)\dot{\varepsilon}_{v}^{p} + f k_{w}\omega\left(\boldsymbol{\sigma}\right)\frac{\boldsymbol{s}\dot{\boldsymbol{e}}^{p}}{\sigma_{e}} \tag{4}$$

where $\dot{\varepsilon}_{v}^{p}$ is plastic volumetric strain rate, k_{w} is a shear state-related constant, ω is a function of a third invariant of stress, and σ_{e} is von-Mises stress.

The plastic deformation of porous PBXs was described by Gurson's theory; and the yield function is,

$$F\left(\sigma_{e}, P, f\right) = \left(\frac{\sigma_{e}}{Y_{M}}\right)^{2} + 2f\cosh\left(-\frac{3P}{2Y_{M}}\right) - f^{2} - 1 \tag{5}$$

The yield strength of the solid material is defined by,

$$Y_M = \left(\sigma_0 + h\bar{\varepsilon}^{p}\right)\left[1.0 + C_1 \ln\left(1+\dot{\varepsilon}^{*}\right)\right] + C_2 P \tag{6}$$

where σ_0 is the initial yield stress; $\bar{\varepsilon}^{p}$ is the effective plastic strain; h is the hardening modulus; C_1 and C_2 are the coefficients of strain rate and pressure.

The shear-crack friction hotspot model used in this study follows that developed by Dienes et al. [9]. The temperature rise due to the frictional heating at shear-crack faces is described as follows:

$$\rho c_v \dot{T}_{cr} = \frac{\partial}{\partial x}\left(k\frac{\partial T_{cr}}{\partial x}\right) + \rho Q_r Z e^{-E/RT_{cr}} + f_m \mu_v \dot{\varepsilon}^2 \tag{7}$$

where T_{cr} is the crack friction hotspot temperature, k is the thermal conductivity, f_m is the melting fraction, and μ_v is the melt viscosity.

Based on the theroy of 1D spherical heat conduction model, a microvoid-collapse-related hotspot model is developed to describe the localized temperature due to void collapse.

$$\rho c_v \dot{T}_{vo} = k\left[\frac{\partial^2 T_{vo}}{\partial r^2} + \frac{2}{r}\frac{\partial T_{vo}}{\partial r}\right] + \dot{w}_{vp}^{*} + \rho Q_r Z e^{-E/RT_{vo}} \tag{8}$$

where T_{vo} is the void collapse hotspot temperature, and the rate of viscoplastic work per unit volume around the void is,

$$\dot{w}_{vp}^{*}\left(r\right) = s_{ij}^{*}\dot{\varepsilon}_{ij}^{*} = \frac{-2Y_M \dot{\varepsilon}_v^{p}}{r^3}\frac{1-f_0}{1-f_{vc}} b_0^3 + \frac{4\eta b^6\left(\dot{\varepsilon}_v^{p}\right)^2}{r^6}\left(\frac{1-f_0}{1-f_{vc}}\right)^2 b_0^6 \tag{9}$$

where a and b are the radii of void and matrix; f_{vc} denotes the part of void fraction related to void collapse; the subscript ‘0’ is the initial state.

4 Results and Discussion

4.1 Computation model

A computation model was designed to study ignition reposnse of PBX9501(95 wt% HMX, 2.5 wt% estane, and 2.5 wt% BDNPA/F) under a complicated impact and shear loading. Namely, a flat-fronted steel rod (Φ20×25mm) normally impacts an uncovered cylindrical explosive charge (Φ60×50mm). Given the axial symmetry of the configuration, only half of the structural geometry model was established using the 2D finite element numerical model. The covergence study displays that the peak stress of Von-Mises histories at region ‘B’ with a mesh size of 0.5mm is only 1.3% larger than the peak value with a mesh of 0.25 mm, which indicates that a mesh size of 0.5mm is sufficiently small to get reasonable results. In the following calculations, all the explosive charges are discretized with a mesh size of 0.5mm. The rod and PBX9501 sample were partitioned by 1000 quad and 12000 triangular elements, respectively. Two regions within the sample labeled by region ‘A’ and ‘B’ are selected to efficiently describe the following analysis. Regions ‘A’ and ‘B’ refer to the center of the sample and the junction between the side of the rod and the sample, respectively. Simulations were performed with an explicit code of Lagrangian finite element named Drexh.

4.2 Distributions of microcrack and microvoid hotspots

Figures 1 and 2 show the contours of microcrack and microvoid-related hotspot temperature (T_{cr} and T_{vo}) under 200 m/s impact. In Fig.1, the area with a relatively high value of T_{cr} (≥ 400 K) mainly gathered around the periphery of the rod front at 5 μs. Ignition (T_{cr} ≥ 750 K) occurs at this area at 10 μs. At the same time, the area undergoing melting (T_{cr}≈ 519 K) formed a semi-ring green zone beneath the rod front. A wedge-shaped zone, which is located between the rod front and melting zone, exhibits few temperature rise caused by friction-locked crack. At 15 μs, ignition area spread along with the boundary of wedge zone and formed a smaller-radius semi-ring red zone, which is defined as transition zone. The cracks in the transition zone underwent a severe frictional heating due to high shear stress. In contrast, from Fig.2, at the top center of friction-locked crack wedge zone (region 'A', $\Delta T_{cr} \approx 0$K), T_{vo} shows a distinct rise ($\Delta T_{vo} \geq 50$ K). The area undergoing a distinct rise of T_{vo} formed an elliptical green zone and propagated following the travel of incident wave front. Non-ignition ($T_{vo} \geq 750$ K) occurs at the whole time due to the insufficient impact strength.

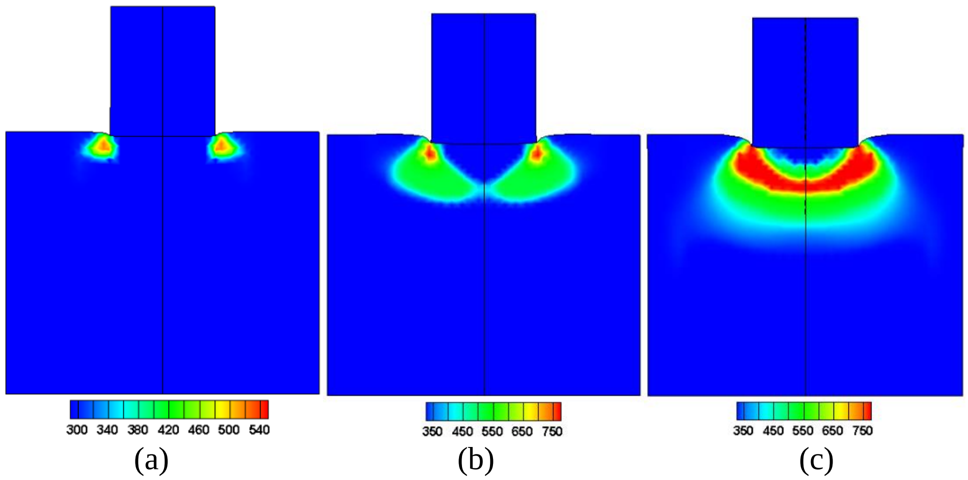

Figure 1 Microcrack-related hotspot temperature contours with 200 m/s impact velocity at (a) 5.0, (b) 10.0, and (c) 15.0 μs.

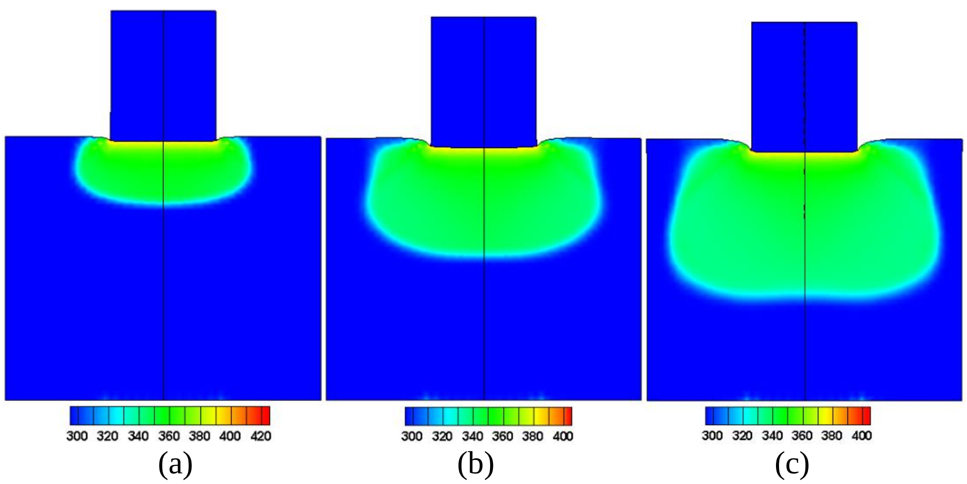

Figure 2 Microvoid-related hotspot temperature contours with 200 m/s impact velocity at (a) 5.0, (b) 10.0, and (c) 15.0 μs.

4.3 Ignition critical velocity related to microcrack and microvoid hotspots

Figure 3(a) and (b) show the evolution of microcrack and microvoid-related hotspot temperature at the riskiest region ('B') with different impact velocities. In Fig. 3(a), at initial impact, the value of T_{cr} shows a rapid rise because high-shear stress at region 'B' contributes to the unstable growth and frictional heating of shear-crack. The hotspot temperature curve for a relatively low-impact (e.g., 125m/s) shows a peak point, indicating that heat generation reaches a maximum and heat conduction begins to control the following behavior. With impact velocity increasing to 150m/s, the peak point disappears and hotspot temperature reaches a plateau corresponding to melting process. After melting, the continual rise of temperature is caused by chemical reaction and intense viscous heating inside molten crack surface. According to run-away feature of the temperature curve, ignition critical velocity due to crack friction (v_{ig_cr}) can be determined as 125-150 m/s.

From Fig. 3(b), T_{vo} first shows a distinct rise at ~0.1µs, corresponding to the accumulation of viscoplastic heating generated from void collapse. If impact velocity is relatively low, heat conduction plays an important role on the change of T_{vo} after the peak point. With impact velocity increasing to 550 m/s, the heat generated from viscoplastic deformation of voids and chemical reaction is larger than the heat loss due to conduction, thereby resulting in the continual rise and final run-away of T_{vo}. Similar to the determination of $v_{ig\text{-}cr}$, ignition critical velocity due to void collapse ($v_{ig\text{-}vo}$) is 300-400 m/s.

From Fig. 3(a), based on the run-away of crack hotspot temperature, time-to-ignition due to crack friction ($t_{ig\text{-}cr}$) is around 27.5µs. And the value of $t_{ig\text{-}cr}$ shows an exponential decrease with increasing impact velocity. Under high-velocity impact (>400 m/s), the heating due to void collapse could induce ignition in a short duration. The time-to-ignition due to void collapse ($t_{ig\text{-}vo}$) is about 3.5µs. Despite the shear-crack heating could also induce ignition at high velocity impact, the duration for shear-crack heating (~10µs) is larger than the duration for void-collapse heating (~1µs). Thus void collapse is the dominant hotspot mechanism under high-velocity impact.

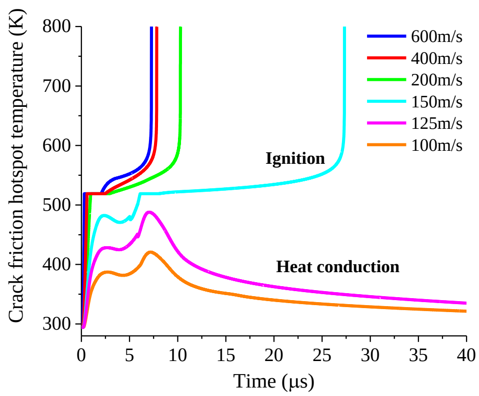

(a)

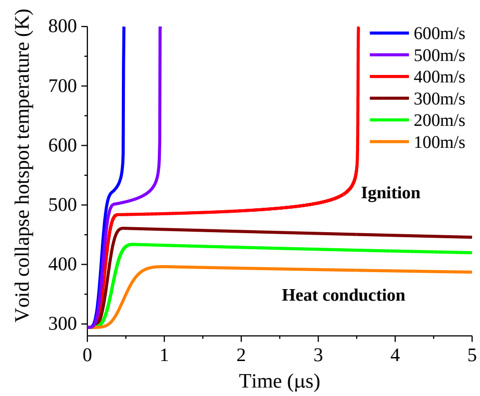

(b)

Figure 3 Evolution of (a) microcrack and (b) microvoid-related hotspot temperature at the riskiest region ('B') with different impact velocities.

5 Conclusions

The modeling of combined microcrack and microvoids related hotspot mechanisms, namely, shear-crack friction heating and viscoplastic heating during void collapse, is chosen to predict ignition response of PBXs. For a punched PBX charge, the simulated results show that shear-crack friction heating plays a critical role on ignition under low-velocity impact (<400m/s). Under high-velocity impact (>400m/s), the heating due to void collapse becomes to dominate ignition since that the time-to-ignition of void hotspots (~1µs) is shorter than the time of crack hotspots (~10µs). At the beneath of rod front (region 'A'), the cracks are stable governed by friction-locked stress state and void collapse becomes a dominant hotspot mechanism.

References

[1] Tarver CM, Chidester SK. (2005). On the violence of high explosive reactions. J. Pres. Vessel. Technol. 127: 39-45.
[2] Field JE. (1992). Hot spot ignition mechanisms for explosives, Acc. Chem. Res. 25: 489-496.
[3] Idar DJ, Straight JW, Osborn MA, et al. Low amplitude impact of damaged PBX 9501. American

Institute of Physics, 2000.
[4] Borne L, Beaucamp A. Effects of explosive crystal internal defects on projectile impact initiation. 12th Detonation symposium. 2002.
[5] Ravindran S, Tessema A, Kidane A. (2017) Multiscale damage evolution in polymer bonded sugar under dynamic loading. Mech. Mater. 114: 97-106.
[6] Wang XJ, Wu YQ, Huang FL. (2017). Thermal–mechanical–chemical responses of polymer-bonded explosives using a mesoscopic reactive model under impact loading. J. Hazard. Mater. 321: 256–267.
[7] Yang K, Wu YQ, Huang FL. (2018). Numerical simulations of microcrack-related damage and ignition behavior of mild-impacted polymer bonded explosives. J. Hazard. Mater. 356: 34–52.
[8] Yang K, Wu YQ, Huang FL. (2019). Microcrack and microvoid dominated damage behaviors for polymer bonded explosives under different dynamic loading conditions. Int. J. Plast. Under Review.
[9] Dienes JK, Zuo QH, Kershner JD. (2006) Impact initiation of explosives and propellants via statistical crack mechanics, J. Mech. Phys. Solids. 54: 1237-1275.